On ionospheric trough conductance and subauroral polarization streams: Simulation results

Yihua Zheng,[1] Pontus C. Brandt,[1] Anthony T. Y. Lui,[1] and Mei-Ching Fok[2]

Received 9 May 2007; revised 8 October 2007; accepted 17 January 2008; published 11 April 2008.

[1] Subauroral polarization streams (SAPS) are usually associated with geomagnetically disturbed times and considered a manifestation of magnetosphere and ionosphere coupling. Previous research results using radar and satellite measurements have revealed many features of the SAPS events. In this paper we focus on the effects of subauroral trough conductance on the attributes of SAPS and the evolution of the coupled magnetosphere and ionosphere system through the comprehensive ring current model, which includes the coupled electrodynamics of the inner magnetosphere and ionosphere with a self-consistent description of the electric field. Our numerical analysis indicates that low conductance at the subauroral latitudes (due to midlatitude trough) is critical to the large amplitude of SAPS. The model results are generally in good agreement with common characteristics of SAPS and are consistent with their existing generation mechanism.

Citation: Zheng, Y., P. C. Brandt, A. T. Y. Lui, and M.-C. Fok (2008), On ionospheric trough conductance and subauroral polarization streams: Simulation results, *J. Geophys. Res.*, *113*, A04209, doi:10.1029/2007JA012532.

1. Introduction

[2] Originally termed polarization jets by *Galperin et al.* [1974], the subauroral ion drifts (SAID) [*Spiro et al.*, 1979; *Anderson et al.*, 2001] refer to the latitudinally narrow (1–2 degrees) regions of rapid westward ion drift (due to poleward directing electric field) located equatorward of the auroral oval. SAID occur predominantly in the premidnight sector, though at times they can have a broad extent (18 MLT – 3 MLT) in magnetic local time (MLT). Latitudinally broader regions of sunward plasma drifts centering at subauroral latitudes have been studied by *Yeh et al.* [1991]. Recently, an inclusive name for these kinds of subauroral sunward plasma convection, Sub-Auroral Polarization Streams (SAPS), has been proposed by *Foster and Burke* [2002] for describing various types of subauroral electric fields. SAPS are the result of the complex interplay between the high-latitude electric field originating from the solar wind and the shielding currents arising from the response of the magnetosphere (mainly the ring current). The distribution of SAPS depends on the structure of the subauroral conductivity structure and the movement of the plasma sheet ion and electron boundaries.

[3] SAPS/subauroral electric fields play an important role in ring current plasma energization and transport, plasmasphere configuration/structuring (e.g., erosion of plasmasphere) and ionospheric dynamics (e.g., storm enhanced density). The characteristics, causes and effects of SAPS have been reported before through particle and field measurements [e.g., *Spiro et al.*, 1979; *Anderson et al.*, 2001; *Foster and Vo*, 2002; *Oksavik et al.*, 2006] and magnetospheric modeling [*Harel et al.*, 1981; *Toffoletto et al.*, 2003; *Garner et al.*, 2004].

[4] A number of SAPS generation mechanisms have been proposed over the years. A detailed description of them can be found in the work of *Anderson et al.* [2001]. The generally accepted picture of SAPS formation is as follows. Large pressure maxima develop in the nightside magnetosphere. Owing to the misalignment between gradients in plasma pressure and magnetic flux tube volume, region 2 field-aligned currents (FACs) flow into the ionosphere in the dusk sector and out of the ionosphere in the dawn sector. In the subauroral ionosphere, where the conductivity is low, region 2 FACs that flow into the region need to be closed via Pederson currents (to maintain current continuity) that direct poleward and therefore result in the poleward electric field that is responsible for the westward flow seen with SAPS. The electric field heating increases the reaction rate of $O^+ + N_2 = NO^+ + N$, and the subsequent rapid recombination rate of NO^+ leads to a greatly reduced ion concentration and the formation of a trough in the region [*Schunk et al.*, 1976]. In return, this will increase the poleward electric field and the frictional heating. The heating leads to thermal expansion, substantial plasma outflow, and further depletion in the F peak concentration, resulting in a reduction of the Pedersen conductance [*Anderson et al.*, 1993] and in the enhancement of SAPS.

[5] The association of SAPS with the midlatitude trough and low subauroral conductance across the region has been recognized [e.g., *Anderson et al.*, 1991]. However, there is still a lack of quantitative analysis of the relationship

[1]Johns Hopkins University Applied Physics Laboratory, Laurel, Maryland, USA.
[2]NASA Goddard Space Flight Center, Greenbelt, Maryland, USA.

Copyright 2008 by the American Geophysical Union.
0148-0227/08/2007JA012532

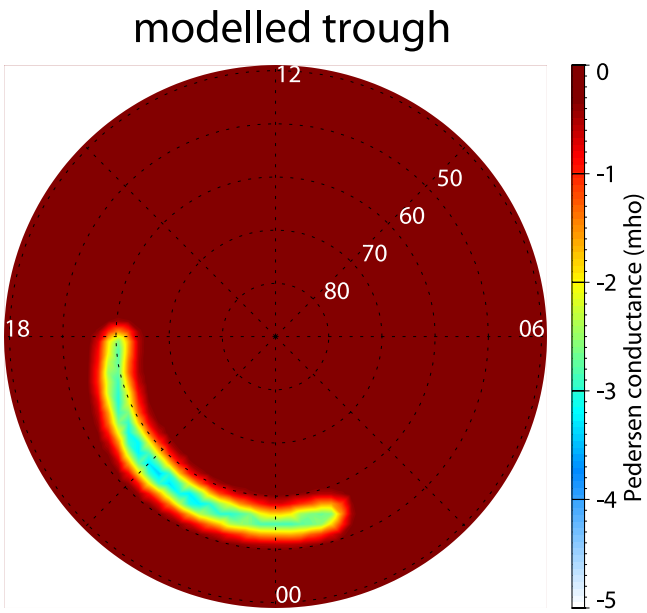

Figure 1. The modeled trough conductance, where the trough minimum latitude is determined from the empirical result of *Spiro* [1978].

between the trough and SAPS. In this paper, we concentrate on the effects of low trough conductance on the dynamics of SAPS and how it subsequently affects the coupled ring current and ionosphere through a global model, namely, the comprehensive ring current model (CRCM).

2. Model Description

[6] The CRCM [*Fok et al.*, 2001] is a simulation code that self-consistently solves the bounce-averaged Boltzmann convection-diffusion equation of ring current particles and the closure of the currents between the inner magnetosphere and ionosphere. As a combination of the Fok et al. ring current model [e.g., *Fok and Moore*, 1997] and Rice Convection Model (RCM) [*Toffoletto et al.*, 2003, and references therein], the CRCM has been successful in modeling the storm time ring current behavior, as well as the dynamics of the coupled ionosphere [e.g., *Ebihara and Fok*, 2004; *Ebihara et al.*, 2005; *Zheng et al.*, 2006]. Details can be found in the work of *Fok et al.* [2001].

[7] The RCM algorithm is used to connect the ring current particles in the magnetosphere to the field-aligned currents in the ionosphere ($J_{||i}$) on the basis of two conservation laws: conservation of number of particles and the current.

[8] The ionospheric Φ_i (therefore the electric field) can be obtained by solving the Poisson equation

$$\nabla \bullet (-\Sigma \bullet \nabla \Phi_i) = J_{||_i} \sin I, \tag{1}$$

where Σ is the height-integrated conductance tensor and I is the magnetic dip angle. The ionospheric electric potential Φ_i calculated by equation (1) is mapped along magnetic field lines using the assumption that the field line is equipotential. The newly updated electric field is then used to solve the kinetic equation of ring current particles.

[9] Even though this paper concerns mostly our simulation results, the solar wind, interplanetary magnetic field (IMF) parameters, and geomagnetic indices for setting up a proper boundary condition/model input that are required by the CRCM (such as setting up the ring current source from the plasma sheet at 10 R_E, the potential distribution at high-latitude boundary, the input parameters for the magnetic field model, the *Kp*-dependent midlatitude trough location, etc.) are based on the measurements of the 12 June 2005 event where substantive SAPS was observed both by SuperDARN midlatitude radars at wallops and by DMSP satellites during the period of 2300 UT – 2400 UT.

[10] We used the T96 magnetic field model [*Tsyganenko*, 1995] to define the external magnetic field parameterized by the solar wind dynamic pressure, the *Dst* index, and the IMF By and Bz. From the observations made at the beginning of the simulation (1500 UT on 12 June 2005), the following input parameters were used for the T96 model: a solar wind dynamic pressure of 4.72 nPa, a *Dst* value of -7.5 nT, IMF By of 10.0 nT, and IMF Bz value of 0.21 nT. The magnetic field was kept constant over time. We believe that our choice of the static magnetic field model does not significantly affect the major results since our focus is on the effects of varying subauroral conductance. The Weimer 2000 model [*Weimer*, 2001] was used to set up the potential distribution at the high-latitude boundary (67° in magnetic latitude). The distribution function of the injected particles is assumed to be Maxwellian and solar wind dependent [*Borovsky et al.*, 1998]:

$$N_{PS}(t) = 0.025 \bullet N_{SW}(t - 3hr) + 0.395. \tag{2}$$

N_{PS} is the plasma sheet density in cm^{-3} and N_{SW} is the solar wind density in cm^{-3}. The plasma sheet temperature was kept as a constant (5 keV) for all the simulation runs. The magnetosphere was assumed to be initially filled with preexisting particles whose distribution function was obtained from measurements of the AMPTE/CCE satellites during quiet time [*Sheldon and Hamilton*, 1993]. The distribution function of the preexisting particles does not significantly affect the result because the preexisting particles will be subject to loss soon after the enhancement of the convection electric field as the newly injected particles occupy the inner magnetosphere.

3. Trough Conductance

[11] The ionospheric conductance Σ includes contributions both from solar irradiance (background) and from the auroral particle precipitation. The International Reference Ionosphere (IRI-95) [*Bilitza*, 1997] and the Mass Spectrometer Incoherent Scatter (MSIS-E90) model are used to calculate the background conductance. The Hardy model is used as a default for calculating the auroral conductance, which is *Kp* dependent [*Hardy et al.*, 1987].

[12] A distinctive feature of the nighttime midlatitude (subauroral) ionosphere is the existence of a latitudinally narrow region of reduced plasma density known as the

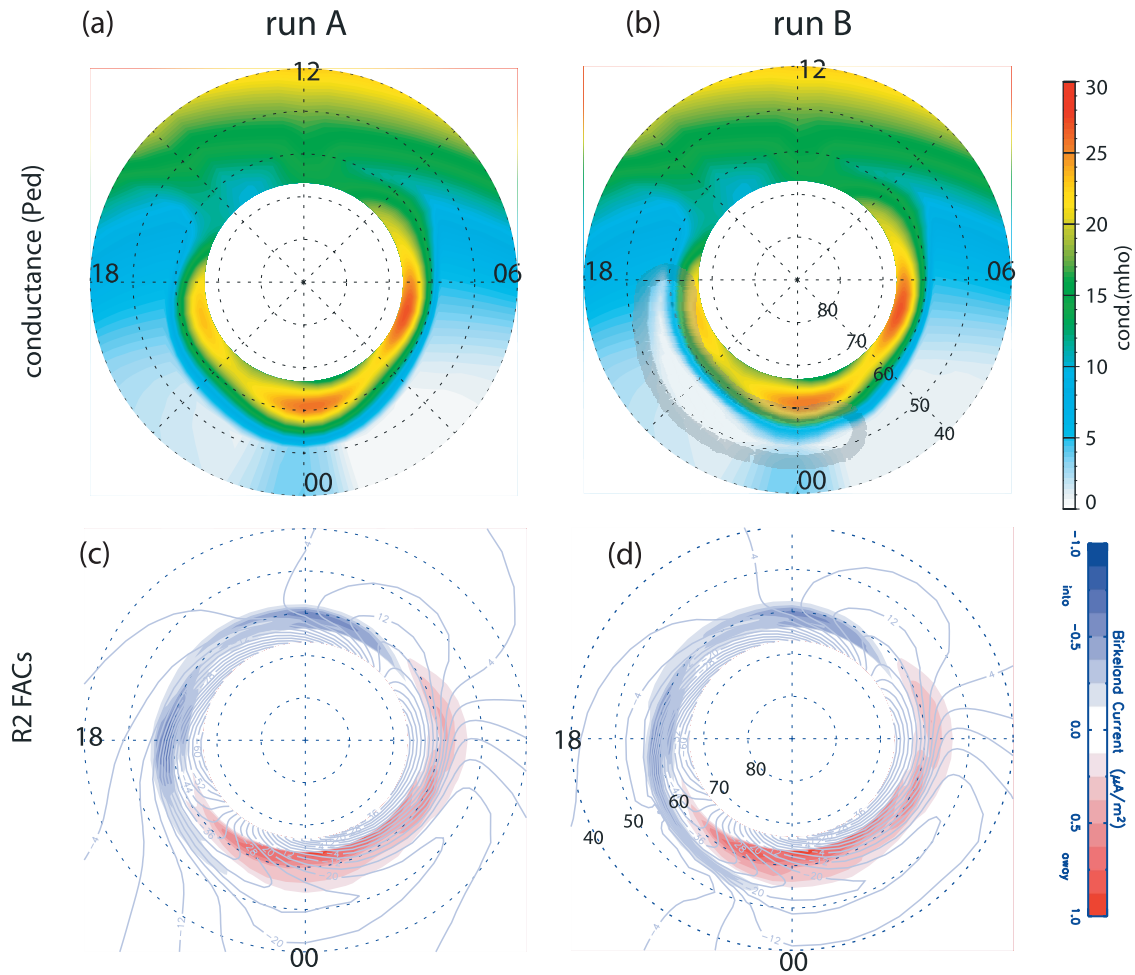

Figure 2. (a, b) The conductance maps and (c, d) the region 2 field-aligned currents (FACs), for the two simulation runs. Figures 2a and 2c are for the run whose conductance includes auroral and solar EUV contributions, while Figures 2b and 2d are for the run whose conductance includes auroral, solar EUV, and the trough conductance that was composed in Figures 1. Noon is at the top, and dusk is to the left.

midlatitude trough [e.g., *Muldrew*, 1965]. SAPS are found to be closely associated with the midlatitude trough and the conductivity distribution in the subauroral ionosphere [e.g, *Anderson et al.*, 1991; *Foster et al.*, 1994]. Since global measurements of the trough and the corresponding height-integrated conductance in the subauroral latitudes are not available, we model it in a simplistic fashion in this paper, providing a starting point for addressing the complex inter-coupling processes involved with the SAPS phenomenon.

[13] To model trough conductance, we first used the empirical relationship derived by *Spiro* [1978] to locate the latitude of trough minimum in 1800–0200 MLT:

$$\Lambda_T = \Lambda_0 + \sum_{n=0}^{3} t^n \left(a_n K_p + b_n\right), \tag{3}$$

where Λ_T is the trough minimum latitude, t is solar local time, K_p is the magnetic activity index, and $\Lambda_0 = 65.45°$, $a_0 = -1.73$, $a_1 = 0.10$, $a_2 = -0.0086$, $a_3 = -0.0017$, $b_0 = 0.00$, $b_1 = -0.80$, $b_2 = 0.099$ and $b_3 = -0.0017$.

[14] Then we applied a Gaussian distribution in latitude for each local time, with the trough conductance taking the following form:

$$cond_{Trough} = -5. * e^{-(\Lambda-\Lambda_T)^2/\Delta\Lambda}. \tag{4}$$

Notice that $cond_{Trough}$ is negative since it will be added to the total conductance to represent the low-conductance region associated with the trough. As seen in equation (3), Λ_T is a function of Kp and MLT. $\Delta\Lambda$ is modeled here as a function of MLT. If we define MLT_d as the MLT in degrees (with 12 MLT as 0°, 18 MLT as 90°, 24 MLT 180°, 6 MLT as 270°), $\Delta\Lambda$ is chosen as follows:

$$\begin{aligned} \Delta\Lambda &= 3. + |MLT_d - 90°| \quad (MLT_d \le 135°), \\ \Delta\Lambda &= 3. + |180° - MLT_d| \quad (MLT_d \le 135°). \end{aligned} \tag{5}$$

This results in $\Delta\Lambda = 6°$ (with a full width of 4.08°) at 21 MLT and $\Delta\Lambda = 3°$ (full width of 2.88°) at 18 MLT and 24 MLT. It should be noted that the major conclusion of this paper is not affected by the choice of $\Delta\Lambda$. Since K_p did not

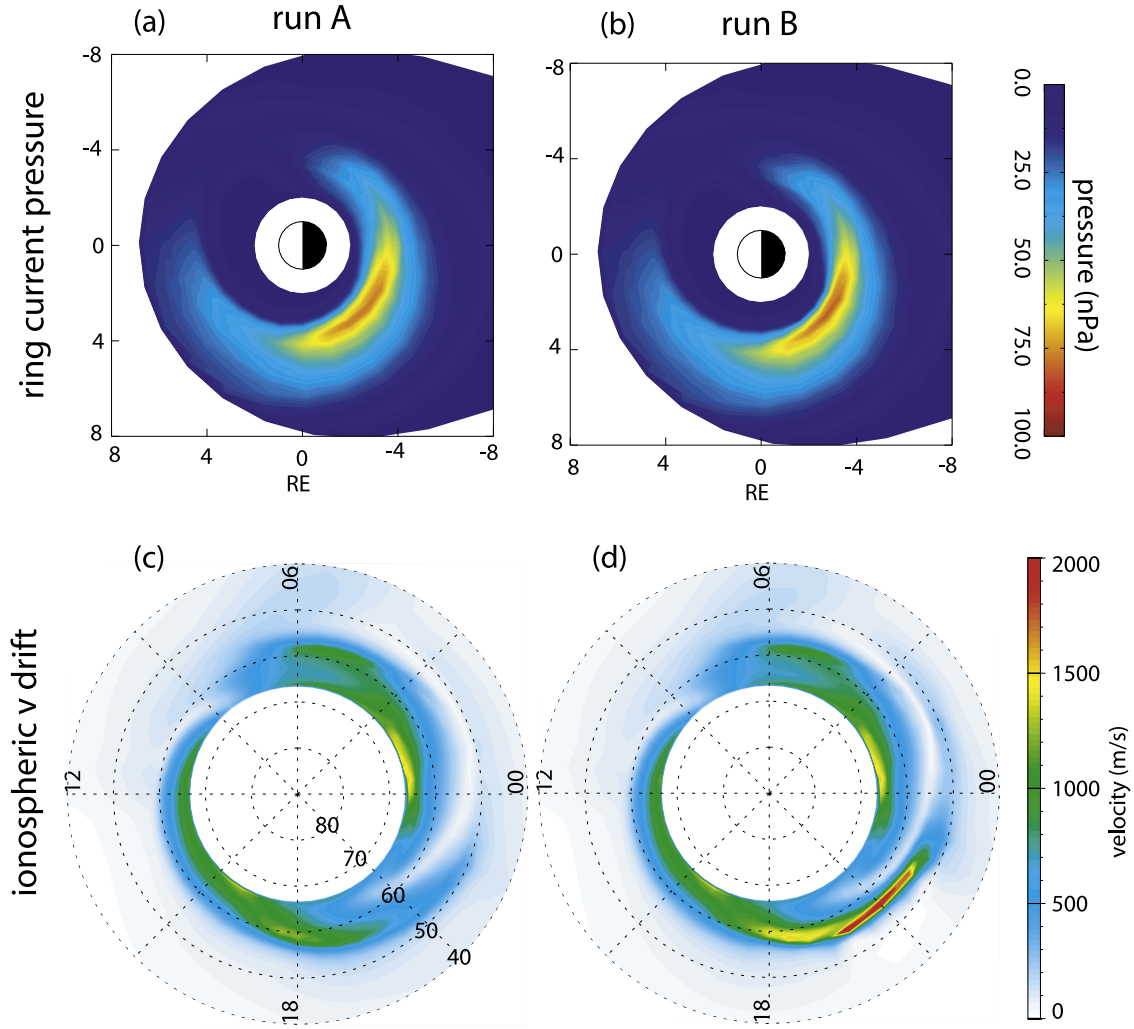

Figure 3. (a, b) The perpendicular pressure of the ring current and (c, d) the ionospheric ion drift, for the two runs. Figures 3a and 3c are for the run without trough conductance, and Figures 3b and 3d are for the run with trough conductance.

change much over our simulation interval (15 – 24 UT on 12 June 2005), we kept it time independent (K_p = 6).

[15] Figure 1 shows our composed trough conductance. Observations suggest that the conductance in the trough region sometimes can be as low as 0.1 mho.

4. Simulation Results

[16] Two simulation runs (run A and run B) are shown in Figure 2, with Figures 2a and 2b showing the conductance map and Figures 2c and 2d showing the region 2 FACs calculated from the model, along with the ionospheric potential pattern. The noon is at the top, and dusk is to the left. Figures 2a and 2c are for the run whose conductance includes auroral and solar EUV contributions (run A), while Figures 2b and 2d are for the run (run B) whose conductance includes auroral, solar EUV, and the trough conductance that was composed in Figure 1. In our simulation, if the combined total conductance is below zero, we set it to be 1.0 mho.

[17] Figure 2 indicates that the addition of a localized low-conductance region due to the trough results in a larger electric field in the region. With a trough, the region 2 FACs that flow into the ionosphere in the dusk sector have a further extension toward midnight and their latitudinal coverage becomes narrower, compared to the one without the trough. But the effects of the trough are limited to the localized regions surrounding it.

[18] Figure 3 shows the perpendicular pressure distribution of the ring current and the magnitude of ionospheric ion drift for two runs, with run A in Figures 3a and 3c and run B with a trough in Figures 3b and 3d. While the difference in ring current perpendicular pressure is small, the ionospheric ion drift has a dramatic difference in the dusk sector.

[19] To have a quantitative assessment of the result, we compared the line plots of a few physical quantities at 21 MLT. Figure 4a shows the result of run A without the trough, and Figure 4b is the result for run B with the trough. Region 2 FACs (in $\mu A/m^2$, downward: positive and upward negative), Pedersen conductance (in mho), and the magnitude of the azimuthal ionospheric drift (in m/s, from $\mathbf{E} \times \mathbf{B}$) are shown from top to bottom. Two other runs (run C and run D) with different trough conductance profiles were also

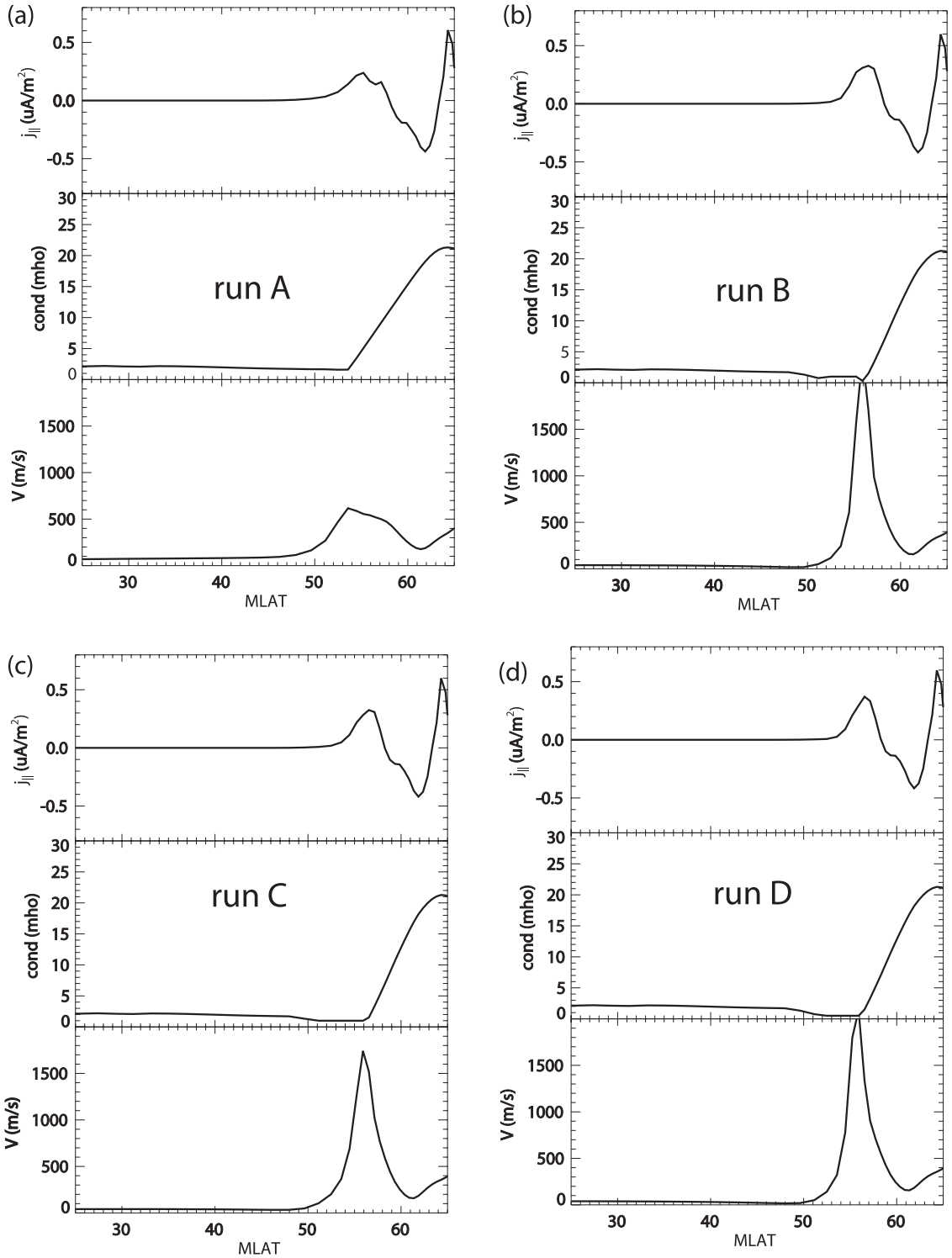

Figure 4. (a, c) The runs without the trough and (b, d) the runs with the trough. Region 2 FACs (downward: positive and upward negative), Pedersen conductance, and the magnitude of the azimuthal ionospheric drift are shown from top to bottom.

performed for comparative analysis. The most striking feature of Figure 4 is the large drift that results from the low-conductance trough region, which maps to 3–4 R_E at the magnetic equator. The latitudinal profile is also similar to the known features of SAPS. Both the minimum trough conductance (over 49°–57° MLAT range) versus the drift velocity maximum (Figure 5a) and the averaged trough conductance versus the drift maximum show a nonlinear relationship (Figure 5b), probably owing to the complex magnetosphere-ionosphere (M-I) coupling. Both the averaged value of trough conductance and its localized minima affect the strength of SAPS. On the basis of our modeling

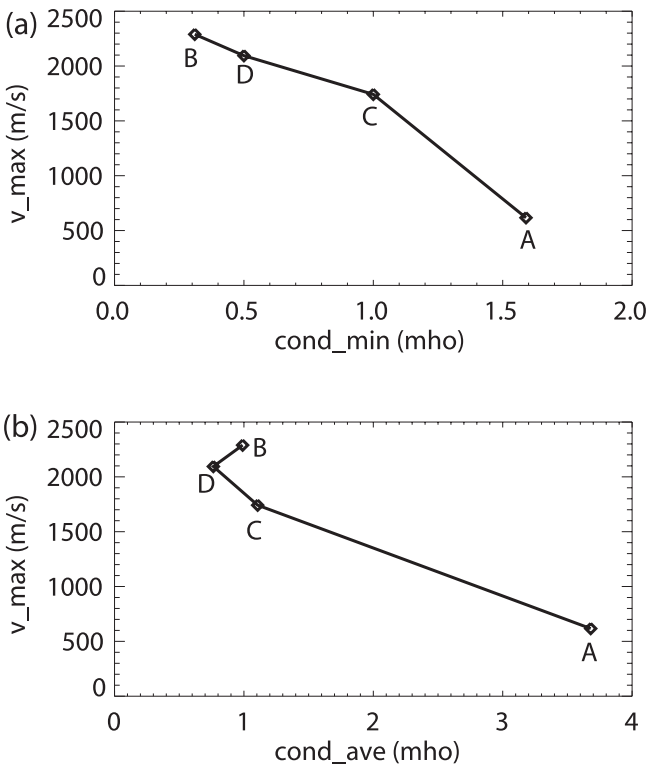

Figure 5. Quantitative analysis of the simulation results, with (a) the relationship between the conductance minimum (over the latitudinal range of 49°–57° magnetic latitude, MLAT) and the drift maximum and (b) the averaged conductance versus the drift maximum. The nonlinear relationship between the trough conductance and the ion drift is evident.

result (with limitations as the trough conductance is taken from an empirical relationship and does not evolve self-consistently with ionospheric dynamics), the low conductance in the trough region acts to prevent the further equatorward penetration of the high-latitude potential drop that is imposed from the solar wind and magnetosphere coupling. But recent studies have shown that the region 2 field-aligned currents sometimes have a very limited shielding effect on the high-latitude electric field, which can penetrate to the low-latitude ionosphere without effective shielding for a few hours [*Huang et al.*, 2005]. It would be interesting to study the evolution of the trough during these long-duration penetration events: the ionospheric conductance may be high overall.

5. Discussion and Summary

[20] In the widely accepted mechanism of SAPS, nightside low conductance equatorward of the auroral oval is responsible for the formation of large subauroral electric fields. But quantitative measures of the relationship are lacking. With consideration of inner magnetosphere and ionosphere coupling, our simulation results show that a latitudinally narrow region of low conductance can have dramatic effects on subauroral electric fields. Therefore the association of the ionospheric trough and SAPS is evident, and resembles what has been observed. Even though our representation of a trough conductance may be simplified, the importance of subauroral conductance from the simulation is demonstrated, which is the intent of this brief report. Other comparative simulation runs with and without trough conductance also lead to the same conclusion. A comprehensive analysis of a large data set (including ion drift measurements from DMSP and SuperDARN Wallops HF radar, IMAGE/HENA data of the ring current, etc.) of this event will be pursued in a separate paper. Our future plan of modeling the effects of the midlatitude trough on the formation of SAPS includes three steps of ascending scope: (1) adopting more realistic conductance value for the trough region, such as the one deduced from the incoherent scatter radar measurements; (2) incorporating some kind of feedback mechanism in a simplistic fashion first, such as allowing the trough conductance to evolve with the electric field; and (3) coupling the CRCM with a self-consistent ionosphere model which includes the complexity of the M-I

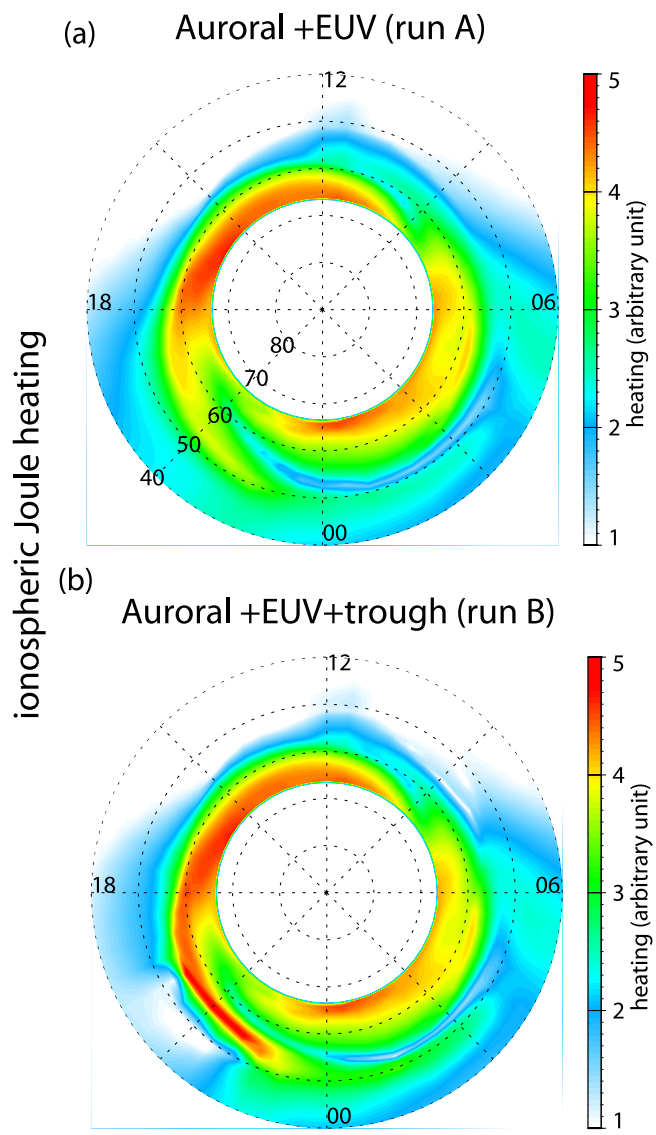

Figure 6. Maps of Joule heating (a) without trough conductance and (b) with trough conductance.

coupling and ionospheric chemistry and dynamics that are involved in the formation and evolution of the trough.

[21] The logarithmic value of Joule heating ($\Sigma_p E^2$) from the two runs (it is in the same arbitrary unit that is equivalent to a watt) is shown in Figures 6a and 6b, showing runs without and with the trough effect in the conductance, respectively. The noon is at the top, and the dusk is to the left. The results indicate that without considering the trough conductance effect, Joule heating in the premidnight sector (18 MLT – 24 MLT) has a wider latitudinal spread and weak intensity (Figure 6a) that contrasts dramatically with the run including a lower conductance in the trough region (Figure 6b). The energy deposited through Joule heating in the trough region may in return enhance the recombination rate and further reduce the conductance.

[22] In summary, our numerical results show that subauroral low conductance can be used as one of the possible explanations of the rapid subauroral ion drifts during disturbed times and its importance should be recognized. A narrow region of reduced conductance at subauroral latitudes can result in a very large increase in the amplitude of SAPS. The locally reduced conductance in the dusk sector causes the inflowing region 2 field-aligned currents to extend further toward midnight but has limited effects on the total plasma pressure of the ring current.

[23] **Acknowledgments.** We wish to thank A. J. Ukhorskiy for helpful discussions related to this study and R. A. Wolf and his coworkers for the development of RCM. This work was supported by NASA grants NNX07AG08G and NNX06AC29G to JHU/APL. We are grateful to the reviewers for their constructive comments.

[24] Amitava Bhattacharjee thanks Phillip Anderson and another reviewer for their assistance in evaluating this paper.

References

Anderson, P. C., W. B. Hanson, and R. A. Heelis (1991), The ionospheric signatures of rapid subauroral ion drifts, *J. Geophys. Res.*, *96*, 5785.

Anderson, P. C., W. B. Hanson, R. A. Heelis, J. D. Craven, D. N. Baker, and L. A. Frank (1993), A proposed production model of rapid subauroral ion drifts and their relationship to substorm evolution, *J. Geophys. Res.*, *98*, 6069.

Anderson, P. C., D. L. Carpenter, K. Tsuruda, T. Mukai, and F. J. Rich (2001), Multisatellite observations of rapid subauroral ion drifts (SAID), *J. Geophys. Res.*, *106*, 29,585.

Bilitza, D. (1997), International reference ionosphere: Status, 1995/96, *Adv. Space Res.*, *20*, 1751.

Borovsky, J. E., M. F. Thomsen, and R. C. Elphic (1998), The driving of the plasma sheet by the solar wind, *J. Geophys. Res.*, *103*, 17,617.

Ebihara, Y., and M.-C. Fok (2004), Postmidnight storm-time enhancement of tens-of-keV proton flux, *J. Geophys. Res.*, *109*, A12209, doi:10.1029/2004JA010523.

Ebihara, Y., M.-C. Fok, S. Sazykin, M. F. Thomsen, M. R. Hairston, D. S. Evans, F. J. Rich, and M. Ejiri (2005), Ring current and the magnetosphere-ionosphere coupling during the superstorm of 20 November 2003, *J. Geophys. Res.*, *110*, A09S22, doi:10.1029/2004JA010924.

Fok, M.-C., and T. E. Moore (1997), Ring current modeling in a realistic magnetic field configuration, *Geophys. Res. Lett.*, *24*, 1775.

Fok, M.-C., R. A. Wolf, R. W. Spiro, and T. E. Moore (2001), Comprehensive computational model of the Earth's ring current, *J. Geophys. Res.*, *106*, 8417.

Foster, J. C., and W. J. Burke (2002), SAPS: A new characterization for subauroral electric fields, *Eos AGU Trans.*, *83*(36), 393.

Foster, J. C., and H. B. Vo (2002), Average characteristics and activity dependence of the subauroral polarization stream, *J. Geophys. Res.*, *107*(A12), 1475, doi:10.1029/2002JA009409.

Foster, J. C., M. J. Buonsanto, M. Mendillo, D. Nottingham, F. J. Rich, and W. Denig (1994), Coordinated stable auroral red arc observations: Relationship to plasma convection, *J. Geophys. Res.*, *99*, 11,429.

Galperin, Y., V. N. Ponomarev, and A. G. Zosimova (1974), Plasma convection in the polar ionosphere, *Ann. Geophys.*, *30*, 1.

Garner, T. W., R. A. Wolf, R. W. Spiro, W. J. Burke, B. G. Fejer, S. Sazykin, J. L. Roeder, and M. R. Hairston (2004), Magnetospheric electric fields and plasma sheet injection to low L-shells during the 4–5 June 1991 magnetic storm: Comparison between the Rice Convection Model and observations, *J. Geophys. Res.*, *109*, A02214, doi:10.1029/2003JA010208.

Hardy, D. A., M. S. Gussenhoven, R. Raistrick, and W. J. McNeil (1987), Statistical and functional representations of the pattern of auroral energy flux, number flux and conductivity, *J. Geophys. Res.*, *92*, 12,275.

Harel, M., R. A. Wolf, R. W. Spiro, P. H. Reiff, C.-K. Chen, W. J. Burke, F. J. Rich, and M. Smiddy (1981), Quantitative simulation of a magnetospheric substorm: 2. Comparison with observations, *J. Geophys. Res.*, *86*, 2242.

Huang, C.-S., J. C. Foster, and M. C. Kelley (2005), Long-duration penetration of the interplanetary electric field to the low-latitude ionosphere during the main phase of magnetic storms, *J. Geophys. Res.*, *110*, A11309, doi:10.1029/2005JA011202.

Muldrew, D. B. (1965), Flayer ionization troughs deduced from Alouette data, *J. Geophys. Res.*, *70*, 26351965.

Oksavik, K., R. A. Greenwald, J. M. Ruohoniemi, M. R. Hairston, L. J. Paxton, J. B. H. Baker, J. W. Gjerloev, and R. J. Barnes (2006), First observations of the temporal/spatial variation of the sub-auroral polarization stream from the SuperDARN Wallops HF radar, *Geophys. Res. Lett.*, *33*, L12104, doi:10.1029/2006GL026256.

Schunk, R. W., P. M. Banks, and W. J. Raitt (1976), Effects of electric fields and other processes upon the nighttime high-latitude F layer, *J. Geophys. Res.*, *81*, 3271.

Sheldon, R. B., and D. C. Hamilton (1993), Ion transport and loss in the Earth's quiet ring current: 1. Data and standard model, *J. Geophys. Res.*, *98*, 13491.

Spiro, R. W. (1978), A study of plasma flow in the mid-latitude ionization trough, Ph.D. dissertation, Univ. of Tex., Dallas.

Spiro, R. W., R. A. Heelis, and W. B. Hanson (1976), Rapid subauroral ion drifts observed by Atmospheric Explorer C, *Geophys. Res. Lett.*, *6*, 657.

Toffoletto, F., S. Sazykin, R. Spiro, and R. Wolf (2003), Inner magnetosphere modeling with the Rice Convection Model, *Space. Sci. Rev.*, *107*, 175.

Tsyganenko, N. A. (1995), Modeling the Earth's magnetospheric magnetic field confined within a realistic magnetopause, *J. Geophys. Res.*, *100*, 5599.

Weimer, D. R. (2001), An improved model of ionospheric electric potentials including substorm perturbations and application to the Geospace Environment Modeling November 24, 1996, event, *J. Geophys. Res.*, *106*, 407.

Yeh, H.-C., J. C. Foster, F. J. Rich, and W. Swider (1991), Storm-time electric field penetration observed at mid-latitude, *J. Geophys. Res.*, *96*, 5707.

Zheng, Y., A. T. Y. Lui, M.-C. Fok, B. J. Anderson, P. C. Brandt, T. J. Immel, and D. G. Mitchell (2006), Relationship between Region 2 field-aligned current and the ring current: Model results, *J. Geophys. Res.*, *111*, A11S06, doi:10.1029/2006JA011603.

P. C. Brandt, A. T. Y. Lui, and Y. Zheng, JHU APL, 11100 Johns Hopkins Road, Laurel, MD 20723-6099, USA. (pontus.brandt@jhuapl.edu; tony.lui@jhuapl.edu; yihua.zheng@jhuapl.edu)

M.-C. Fok, NASA Goddard Space Flight Center, Code 612.2, Greenbelt, MD 20771, USA. (mei-ching.h.fok@nasa.gov)